Bioelectrochemistry 154 (2023) 108527

Contents lists available at ScienceDirect

Bioelectrochemistry

journal homepage: www.journals.elsevier.com/bioelectrochemistry

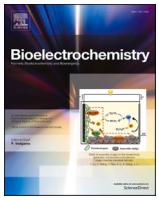

Probing electrophysiological activity of amphiphilic Dynorphin A in planar neutral membranes reveals both ion channel-like activity and neuropeptide translocation

Laidy M. Alvero-Gonzalez [a,1], D. Aurora Perini [a,1], María Queralt-Martín [a], Alex Perálvarez-Marín [b,c,*], Clara Viñas [d], Antonio Alcaraz [a,*]

[a] Laboratory of Molecular Biophysics, Department of Physics, University Jaume I, 12071 Castellón, Spain
[b] Biophysics Unit, Department of Biochemistry and Molecular Biology, School of Medicine, Universitat Autònoma de Barcelona, 08193 Cerdanyola del Vallès, Spain
[c] Institute of Neuroscience, Universitat Autònoma de Barcelona, 08193 Cerdanyola del Vallès, Spain
[d] Institut de Ciència de Materials de Barcelona, ICMAB-CSIC, Campus Universitat Autònoma de Barcelona, 08193 Bellaterra, Spain

ARTICLE INFO

Keywords:
Bilayer lipid membrane
Peptide
Membrane transport
Electrophysiology

ABSTRACT

Dynorphin A (DynA) is an endogenous neuropeptide that besides acting as a ligand of the κ-opioid receptor, presents some non-opioid pathophysiological properties associated to its ability to induce cell permeability similarly to cell-penetrating peptides (CPPs). Here, we use electrophysiology experiments to show that amphiphilic DynA generates aqueous pores in neutral membranes similar to those reported previously in charged membranes, but we also find other events thermodynamically incompatible with voltage-driven ion channel activity (i.e. non-zero currents with no applied voltage in symmetric salt conditions, reversal potentials that exceed the theoretical limit for a given salt concentration gradient). By comparison with current traces generated by other amphiphilic molecule known to spontaneously cross membranes, we hypothesize that DynA could directly translocate across neutral bilayers, a feature never observed in charged membranes following the same electrophysiological protocol. Our findings suggest that DynA interaction with the cellular membrane is modulated by the lipid charge distribution, enabling either passive ionic transport via membrane remodeling and pore formation or by peptide direct internalization independent of cellular transduction pathways.

1. Introduction

Although DynA canonical function is being substrate for the κ-opioid receptor [1], this peptide has a non-opioid physiological activity [2] that can result in neurodegeneration and neuronal death [3]. The pathophysiological mechanisms of DynA could be mediated by non-opioid receptors [1,4,5] or by peptide-induced changes in membrane morphology [6]. In a recent study we used electrophysiology in planar bilayers to show that DynA induces the formation of aqueous pores in negatively charged membranes with a notable diversity of conducting levels and lifetimes [7]. Remarkably, the fact that positively charged DynA peptides induce cation-selective pores indicates that negative lipid charges are necessarily involved in the channel structure [8,9]. Subsequent MD simulations demonstrated how the interaction of several peptides with negatively charged phosphatidylserine (PS) molecules allows the proteo-lipidic structure to stabilize towards the hydrophobic core forming a water-filled pore able to conduct ions [7].

DynA shares common properties with the so-called Cell Penetrating Peptides (CPP) [2,10] such as having short amino acid chains with a high content of basic residues (see Materials and Methods for DynA sequence) [11,12] and displaying the ability to penetrate into membranes, even translocating themselves and/or delivering a wide variety of cargos into cells [13,14]. Indeed, the ability of CPPs to cross living cells, either by means of energy-independent (the so-called direct translocation) or by energy-dependent mechanisms (endocytosis) has been a matter of intense debate [15–17]. Note that in this context, the

* Corresponding authors at: Biophysics Unit, Department of Biochemistry and Molecular Biology, School of Medicine, Universitat Autònoma de Barcelona, 08193 Cerdanyola del Vallès, Spain (A. Perálvarez-Marín); Laboratory of Molecular Biophysics, Department of Physics, University Jaume I, 12071 Castellón, Spain (A. Alcaraz).
E-mail addresses: alex.peralvarez@uab.cat (A. Perálvarez-Marín), alcaraza@uji.es (A. Alcaraz).
[1] These authors contributed equally.

https://doi.org/10.1016/j.bioelechem.2023.108527
Received 26 May 2023; Received in revised form 10 July 2023; Accepted 26 July 2023
Available online 26 July 2023

term "direct translocation" specifically pertains to a mechanism that operates independently of cellular machinery. However, it does not imply the absence of changes in molecule structure or dynamics, self-association or interactions with the lipid. In fact, as elaborated later in the paper, it is expected that several of these properties would undergo significant alterations to accommodate spontaneous transport. Although evidence of DynA direct translocation has been already reported using techniques such as confocal fluorescence microscopy/immunolabeling and linked to interneuronal communication [18], no electrophysiological evidence of it was found in our previous study in charged membranes [7]. Here, we extend our investigation with DynA to neutral phosphatidylcholine (PC) membranes where, besides membrane poration similar to that found in PS, we detected the existence of uncorrelated fluctuations patterns in noise analysis and other events non-compatible with voltage driven ion channel activity, namely the apparition of current without the need for applied voltage in symmetrical conditions, and also measured reversal potentials that exceed the theoretical limit established by Nernst potential. Recently [19], it has been reported that the anionic small metallacarborane cobaltabis (dicarbollide) molecule (abbreviated as [*o*-COSAN]$^-$) displays surfactant behavior without a head and tail design. By comparison with electrophysiological recordings of this amphiphilic [*o*-COSAN]$^-$ molecule that is experimentally known to cross membranes spontaneously by a mechanism kinetically controlled by membrane partition [20], we show that our results are consistent with direct translocation of DynA molecules across the lipid membrane.

2. Materials and Methods

2.1. Planar bilayer formation and electrical measurements

Planar membranes were obtained by apposition of two monolayers in a Teflon chamber separated in two 1.6 mL compartments (so-called *cis* and *trans*) by a 15 μm-thick Teflon film with a 70–100 μm diameter orifice, using a modified solvent-free Montal-Mueller technique [21,22]. In brief, the lipid was prepared by dissolving diphytanoylphosphatidylcholine (PC) (Avanti Polar Lipids, Inc., Alabaster, AL) in pentane at 5 mg/mL after chloroform evaporation. Aliquots of 10–20 μL of lipid in pentane were added onto salt solution subphases at both the *cis* and *trans* compartments. The orifice was pretreated with a 1% solution of hexadecane in pentane. After pentane evaporation, the level of solutions in each compartment was raised above the hole so that the planar bilayer was formed by monolayer apposition. pH of salt solutions was adjusted by adding HCl, KOH (for KCl solutions) or NaOH (for NaCl solutions) and monitored during experiments with a GLP22 pH meter (Crison).

DynA peptides in HCl salt with sequence Tyr-Gly-Gly-Phe-Leu-Arg-Arg-Ile-Arg-Pro-Lys-Leu-Lys-Trp-Asp-Asn-Gln were purchased from Pepmic Co. (Suzhou, China) in powder and dissolved in MilliQ® water. DynA-induced currents were achieved by adding 1–50 μL of a 500 mg/mL solution of DynA peptides at the *cis* or *trans* (in separate experiments) side of the chamber, which corresponds to a DynA peptide final concentration of 0.31–15 mg/mL. The sodium salt of the anionic small metallacarborane cobaltabis(dicarbollide) molecule ([*o*-COSAN]$^-$) was synthesized as reported previously [23]. [*o*-COSAN]$^-$ is an inorganic, icosahedral boron cluster negatively charged molecule with chemical formula ($Na[3,\dot{3}–Co(1,2\text{-}C_2B_9H_{11})_2]$) (see Figure S2 for a schematic representation of the molecule). [*o*-COSAN]$^-$ was dissolved in MilliQ® water at a stock concentration of 10 mM and added to the *cis* side of the chamber to a final concentration of 100 μM. Supplementary Table S1 shows a comparison of basic physicochemical properties for both compounds, DynA and [*o*-COSAN]$^-$.

An electric potential was applied using Ag/AgCl electrodes in 2 M KCl, 1.5% agarose bridges assembled within standard 250 μL pipette tips. The potential was defined as positive when it was higher on the *cis* side, whereas the *trans* side was set to ground. An Axopatch 200B amplifier (Molecular Devices, Sunnyvale, CA) in the voltage-clamp mode was used to measure the current and the applied potential. Current was filtered with a 10 kHz 8-pole in-line Bessel filter and digitized with a Digidata 1440A (Molecular Devices, Sunnyvale, CA) at 50 kHz sampling frequency. For better visualization, all traces shown in this manuscript were further filtered with a digital 500 Hz 8-pole Bessel filter before representation. The membrane chamber and the head stage were isolated from external noise sources with a double metal screen (Amuneal Manufacturing Corp., Philadelphia, PA).

2.2. Current fluctuation analysis

The power spectral density (PSD) of current fluctuations was obtained directly from the measured current traces with the pClamp 10.7 software (Molecular Devices, LLC.). The power spectrum generates a frequency domain representation of the time domain data, revealing the power levels of different frequency components in the signal. PSD was measured by calculating the Fast Fourier Transform from the digitized signal. The PSD spectral resolution used was 0.76 Hz and, for each signal, the available spectral segments were averaged. PSD voltage-dependence was assessed by averaging in the 5–15 Hz (DynA experiments) or 1–4 Hz ([*o*-COSAN]$^-$ experiments) band the obtained PSDs at each applied potential. Only traces in which the current histogram could be represented by a single peak for each applied voltage, were used. When analyzing traces with a non-zero current at $V = 0$, only fragments with the same baseline current were analyzed together.

2.3. Ion selectivity measurements

The cation versus anion preference of DynA-induced currents was assessed by measuring the reversal potential (RP), defined as the applied voltage needed to precisely cancel the current measured when a given salt concentration gradient is applied to the system. For these RP experiments, PC planar membranes were formed under a salt concentration gradient (100/500 mM, or 500/100 mM or 200/100 mM), and the molecule of interest (DynA or [*o*-COSAN]$^-$) was added to the *cis* side of the membrane. The net ionic current obtained was manually set to zero by adjusting the applied potential. This potential was then corrected by the liquid junction potential of the electrode salt bridges [24–26] to obtain the RP.

3. Results and discussion

3.1. DynA peptides induce a variability of currents in neutral bilayers

Once the PC neutral bilayer was formed and its impermeability was checked, DynA peptides were added to the solution, either at the *cis* or *trans* side of the membrane. A significant part of the current observed in symmetrical salt conditions was voltage-driven similar to that found in PS membranes [7], showing a diversity of conductive levels (see Fig. 1) with random transitions between open and closed states (Fig. 1A), somewhat stable albeit noisy currents (Fig. 1B) or successive channel insertions (Fig. 1C) were also recorded. Traces in Fig. 1 were selected from a large number of separate experiments, although it was possible to obtain the different types of currents interchangeably during the same experiment. Usually, after more stable currents like the one in Fig. 1B arose, membrane had to be reformed to obtain again a non-conducting membrane, then apply voltage and wait for new events to appear.

However, additional assays yielded non-zero currents with no applied potential ($V = 0$), so that the recorded currents were positive (Fig. 2 A-B) when DynA was added only to the *cis* side of the chamber and negative (Fig. 2 C-D) when added to the *trans* side. Interestingly, these current traces do not correspond to the progressive membrane disintegration characteristic of the so-called "detergent effect" of peptides disrupting the lipid packing [27,28]. On the contrary, a variety of current levels was found: variable multilevel (Fig. 2 A-C) or stepwise

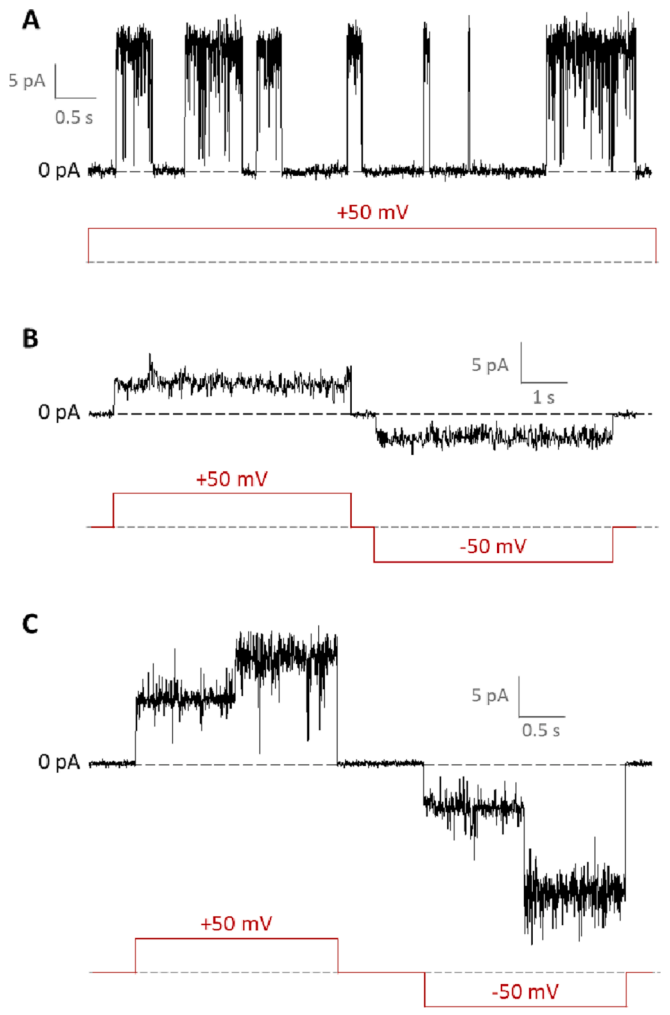

Fig. 1. DynA induces pore formation in neutral membranes. Representative current versus time traces of DynA peptide showing a variety of currents recorded at ±50 mV, as indicated below each trace. **(A)** Noisy currents with fast flickering between two conductance levels obtained at positive voltage. **(B)** More stable currents with well-defined conductance levels independent of polarity. **(C)** Step-like currents recorded at both positive and negative applied voltages. Solutions consisted of 150 mM KCl buffered with 5 mM HEPES at pH 7.4, membrane formed of PC lipid.

currents resembling successive channel insertions and retractions (Fig. 2 B-D). Remarkably, this type of currents were never obtained with charged membranes [7]. Given the thermodynamic impossibility of acquiring non-zero current when V = 0 in passive pores separating symmetric solutions [29,30], we hypothesize that the origin of the events depicted in Fig. 2 lies on the asymmetric addition of DynA (only in one cell side) so that the peptide could become a charge carrier crossing the membrane. We base this conjecture on DynA translocation already reported in the plasma membrane of neuronal and non-neuronal cells using confocal fluorescence microscopy/immunolabeling [10] as commented before. At this point we may wonder whether the amount of DynA added in our protocol (several μl of 500 mg/ml DynA solution is about 10^{17} DynA molecules) is compatible with the transferred charge Q shown in traces of Fig. 2. For instance, Fig. 2A yields Q ~ 300 pC (calculated as the integral of the current over time), which would roughly corresponds to 10^9 DynA translocating molecules, a number considerably lower that the added amount of DynA. Note however, that our hypothesis raises some questions. On the one side, if the currents in Fig. 2 are carried exclusively by peptides, it suggests a strong cooperative behavior of DynA molecules during translocation, either in form of self-aggregation or via DynA/lipid structures able to induce transient membrane defects. On the other side, our results cannot discriminate between current carried by proteins and salt ions, so that it is possible that protein translocation could involve the simultaneous formation of conducting structures in which salt ions are dragged together with the peptides. In fact, the coexistence of both mechanisms might explain the striking resemblance between traces in Fig. 1 and Fig. 2.

3.2. *Noise analysis of current traces shows events compatible with uncorrelated fluctuations*

DynA-induced currents contain additional information other than ionic conductance, namely information coming from the open channel noise analysis that we examine via the power spectral density (PSD) of recorded currents. The exploration of the frequency-dependence of PSD in the context of membrane transport is extremely complex because several mechanisms can potentially generate similar PSD [31,32], such as random diffusion processes [33], transitions between conductive states [34,35] and also self-organized criticality [36]. In view of that, we focus here only on how the calculated PSDs depend on applied voltage (and hence in current) in relatively quiet traces (current histograms can be represented by a single peak, see Materials and Methods) that provide a clear I-V relationship (this is not possible in traces with highly dynamic behavior).

The different panels in Fig. 3 display I-V curves, the corresponding PSDs and how the low frequency band of these PSDs depends on I, for experiments carried out in neutral membranes where non-zero currents were observed at V = 0. DynA-induced spontaneous currents at V = 0 were I > 0 when DynA was added only to the *cis* side (upper panel A), whereas I < 0 was found when the protein was added only to the *trans* side (lower panel B). The application of voltage leads to approximately ohmic I-V curves and 1/f spectra are observed for the PSD in the low frequency limit. Interestingly, PSDs are current-independent ($PSD/I^2 \sim 1/I^2$) indicating that these spectra correspond to uncorrelated fluctuations [37,38]. This suggests that the PSD contains different sources of noise that are not interdependent, as could be the mechanism underlying the spontaneous DynA translocation and the voltage-driven transport superimposed over it.

Other DynA-induced currents yielded 1/f-like spectra with an averaged PSD at low frequencies showing a roughly parabolic dependence on I, which is more similar to the results obtained in charged membranes [7]. This behavior is characteristic of equilibrium correlated fluctuations [35,37,39,40].

3.3. *Ion selectivity experiments yield anion- and cation-selective pores and voltages exceeding the Nernst theoretical limit*

To further characterize DynA-induced currents in neutral membranes, the ionic selectivity was obtained by measuring the reversal potential (RP) (see Materials and Methods) in experiments involving a 5-fold KCl concentration gradient across the membrane. As shown in Fig. 4, measurements in neutral lipid show considerable dispersion in comparison with the data obtained for DynA in charged membranes [7]. Measured RP in PC goes from a minority showing anionic preference (in agreement with the peptide positive net charge) up to a majority compatible with cationic selectivity (Fig. 4A and Fig. 4B). Such preference for cations is hard to reconcile with proteolipidic pores formed by basic peptides and neutral lipids. Furthermore, certain RP values exceed the corresponding Nernst potential [41,42] for a 5-fold concentration gradient (Fig. 4C). Again, thermodynamic limits urge to consider alternatives to purely diffusive salt transport across membrane pores, pointing to DynA translocation across the membrane. The spontaneous transport of DynA positively charged peptides from the side of addition to the other side would account for the observed cationic selectivity, and would explain why this transfer of charge is not affected by the Nernst limit corresponding to the salt concentration gradient.

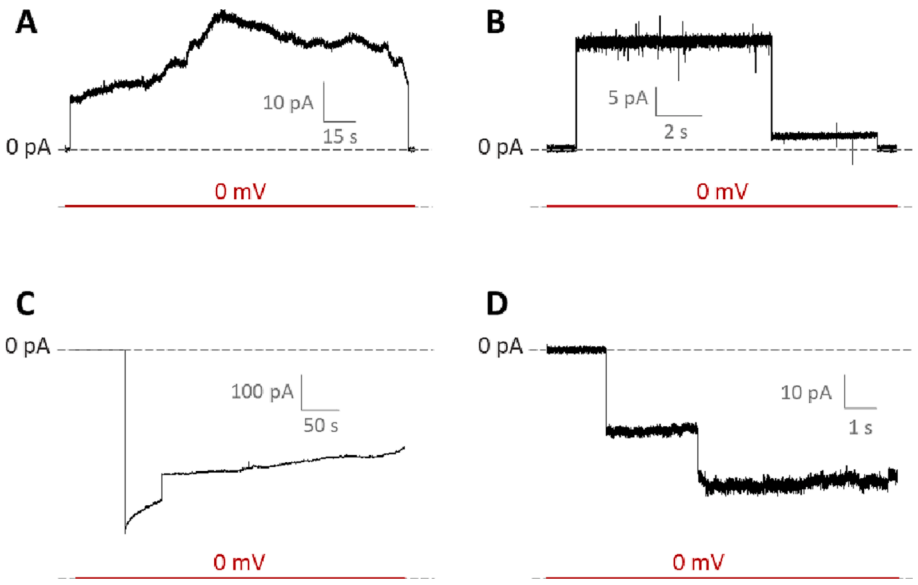

Fig. 2. DynA induces currents with no applied voltage in neutral membranes. (A-B) Positive recorded currents and **(C-D)** negative recorded currents showing multilevels (A–C) as well as step-like transitions (B–D). Experimental conditions as in Fig. 1, except for the voltage, which was always 0 mV, as indicated below each trace.

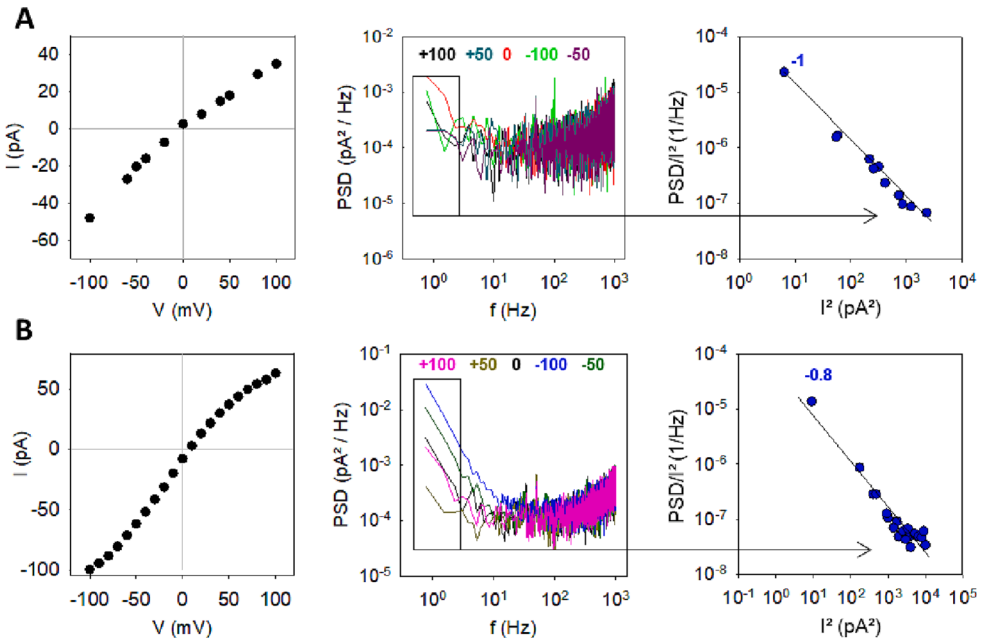

Fig. 3. DynA-induced currents in neutral membranes can show uncorrelated noise. Current-voltage curve (*left panels*), PSDs (*center panels*) and relative averaged noise amplitude (PSD/I^2) vs square of the current (I^2) (*right panels*) from spontaneous positive **(A)** and negative **(B)** DynA-induced currents. Experimental conditions as in Fig. 2. Corresponding current traces are shown in Supplementary Fig. S1. In the center panels, colored numbers indicate the applied potential for each PSD in millivolts. In the right panels, numbers indicate the exponent of a power fitting (solid lines) of the experimental data (blue circles). An exponent close to 1 indicates that $PSD/I^2 \sim 1/I^2$ and therefore the PSDs are current-independent.

3.4. Amphiphilic [o-COSAN]⁻ provides an electrophysiological fingerprint of direct translocation across the planar membrane

The translocation of protein peptides has been assessed in vesicles and liposomes using different methods involving fluorescence or FRET [43,44]. However, such methodologies or conventional analytical techniques are extremely difficult to combine with electrophysiology at the single peptide level due to the low number of molecules involved. For this reason, we use as a case study the interaction between [*o*-COSAN]⁻ and planar phospholipid membranes that are prepared using the same procedure as that used in the electrophysiological experiments described above. The reason to use this boron-based molecule is that in resemblance to DynA, [*o*-COSAN]⁻ is amphiphilic, but in contrast to DynA, after [*o*-COSAN]⁻ addition in one side of the chamber separating a planar membrane, [*o*-COSAN]⁻ concentration in the other side can be determined by inductively coupled plasma mass spectrometry (ICP-MS) [20], directly demonstrating its translocation. Using [*o*-COSAN]⁻ in different salts it was shown that in all cases the permeation rate was independent of the initial concentration (which in all experiments was 100μM or higher) without affecting membrane integrity [20]. Such zero-order kinetics suggests that translocation could occur via the sequence of absorption at the solution–membrane interface, movement across the lipid phase and desorption at the membrane– solution interface, being the rate-determining step the partitioning of [*o*-COSAN]⁻ into the lipid phase and not [*o*-COSAN]⁻ diffusion [20].

Interestingly, [*o*-COSAN]⁻ translocation shows all characteristics incompatible with voltage-driven transport across passive pores mentioned in previous sections dealing with DynA in neutral

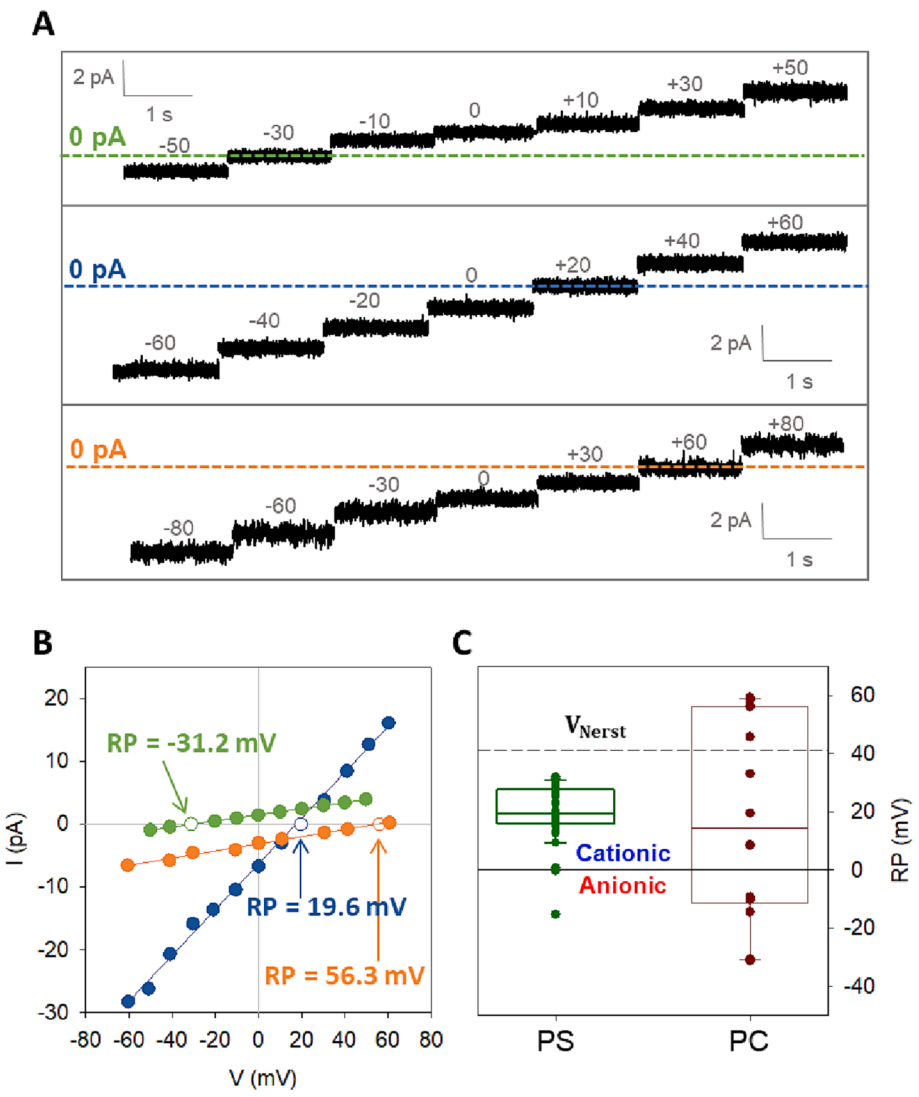

Fig. 4. DynA selectivity experiments yield a high variability of results. (A) Representative traces of DynA-induced currents obtained in PC membranes displaying anionic selectivity (upper trace, RP = -31.2 mV), cationic selectivity (middle trace, RP = 19.6 mV) and a reversal potential that exceed the theoretical Nernst limit (lower trace, RP = 56.3 mV). The dashed line indicates the zero-current level. The applied voltage in millivolts is shown above each piece. (B) Current vs voltage curves of the traces shown in (A). (C) Box plot showing the reversal potential of DynA-induced pores in different lipid compositions. Data for PS reported in [7]. The boundary of the box closest to zero indicates the 25th percentile, a line within the box marks the median, and the boundary of the box farthest from zero indicates the 75th percentile. Error bars indicate SD (n = 49 for PS and n = 14 for PC). The dashed line indicates the theoretical limit (V_{Nernst}) and the solid line shows the threshold between anionic and cationic selectivity. In all panels, solutions consisted of a 5-fold gradient of KCl (100 mM/500 mM KCl) buffered with 5 mM HEPES at pH 7.4.

membranes. As shown in Fig. 5A, [*o*-COSAN]$^-$-induced currents appear without the need of an applied voltage as a result of the asymmetric addition of the molecule. Also, when voltage is superimposed to the spontaneous transport to obtain an I-V curve, the corresponding PSDs show 1/f-like spectra (Fig. 5B). In addition, the low frequency band of normalized PSDs (red circles in Fig. 5C) point to uncorrelated noise in agreement with DynA in PC membranes (blue points) and in contrast with correlated noise characteristic of DynA in PS membranes (green points) previously reported [7]. As for the nature of uncorrelated fluctuations in [*o*-COSAN]$^-$, we interpret this pattern as the coexistence of two independent noise sources, one independent of the concentration of current carriers (zero-order kinetics) and other that depends linearly on carrier concentration (drift generated by applied voltage). As regards selectivity experiments, when negatively charged [*o*-COSAN]$^-$ is added in presence of a concentration gradient in neutral membranes, RP measurements become inconsistent because they suggest anion selective pores without the presence of any positive charges (black dots in Fig. 5D) or even the measured RP surpasses the corresponding Nernst potential (red dots in Fig. 5D).

Note also that the sodium salt of [*o*-COSAN]$^-$ is soluble both in water and oils because of its amphiphilic nature at the price of involving huge conformational changes in terms of structure and self-association, as shown by transmission electron cryomicroscopy (CryoTEM) measurements [20]. In view of the similarities between [*o*-COSAN]$^-$ and DynA, we may wonder whether DynA translocation actually involves similar steps to those proved for [*o*-COSAN]$^-$. Interestingly, atomistic simulations of α-helical peptides with different lengths and amphiphilicity suggest a similar itinerary for translocation peptides: adsorption to the membrane interface / tilting to reach transmembrane orientation / adsorption to the second leaflet [45]. Along this process, it is shown how there is an optimal ratio of hydrophilic/hydrophobic content that allows peptides to translocate the easiest [45]. In addition, experimental and theoretical studies provide evidence that DynA peptide is likely unfolded in an aqueous environment, but it adopts a stable α-helical conformation in the membrane with a tilted orientation that may facilitate DynA translocation in particular conditions [4,46–49]. Also, as mentioned in the discussion of Fig. 2, it is important to consider that the translocation of DynA probably involves a strong cooperative behavior of DynA molecules. In this sense, it has been reported that the self-assembly of amphiphilic peptides leads to a variety of nanostructures that are stabilized in water in form of nanotubes by hydrogen bonding and in membrane environment by the hydrophobic effect yielding micelles [50].

As noted before, the events compatible with DynA translocation in neutral membranes were never observed in charged membranes following the same protocol [7]. In this sense, recall that MD simulations emphasized the crucial role of negatively charged lipids in forming stable proteo-lipidic structures together with the positively charged DynA peptides [7]. We might speculate that neutral lipids are less

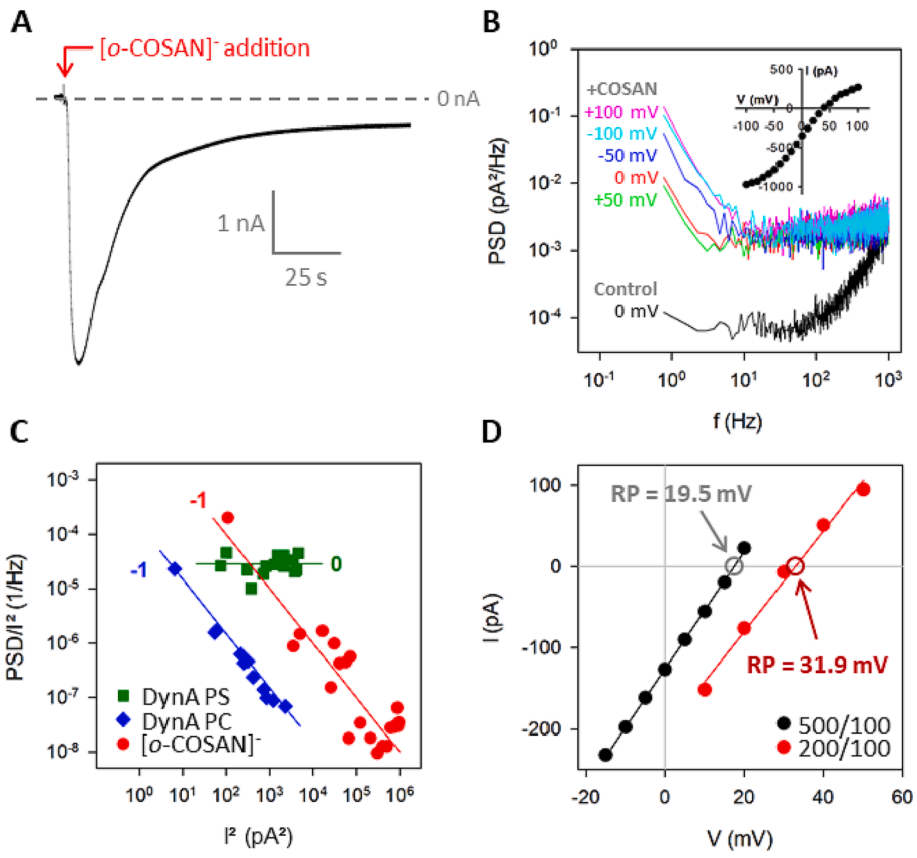

Fig. 5. Electrophysiological fingerprint of [o-COSAN]$^-$ translocation across the planar membrane. (A) Representative current trace obtained after 100 μM [o-COSAN]$^-$ addition to the cis side of the membrane with no applied voltage. Right after addition, there is a peak of negative current, then the current decreases until it stabilizes at a negative value after some minutes. Traces were filtered with a 500 Hz 8-pole Bessel filter. The solutions were prepared using symmetrical 10 μM NaCl at pH 6, which were the same as those utilized in [20]. (B) PSDs of current traces at different applied voltages after [o-COSAN]$^-$ addition at the same conditions as in (A). Data were acquired at least 20 min after addition to assure a steady zero-voltage current. The inset shows the corresponding I-V curve. (C) Relative averaged noise amplitude (PSD/I^2) vs square of the current (I^2) for [o-COSAN]$^-$ (red circles, same conditions as in A,B), DynA in PC membranes (blue diamonds, same data as in Fig. 2A) and DynA in charged PS membranes (green squares, reported in [7]). (D) Reversal potential experiments after the addition of 100 μM COSAM to the cis side of the membrane in two different salt conditions: 500 mM/100 mM NaCl (black) and 200/100 NaCl (red), pH 6. The RP is highlighted for each curve. Solid lines are linear fittings of the experimental data.

capable to stabilize the DynA-induced pores and hence facilitate the peptide translocation. However, this intuitive reasoning could seem insufficient in view of the extended leakage studies of DynA indicating that peptide-membrane interactions are ruled by a complex interplay of factors such as membrane composition, peptide hydrophobicity, total charge and number of arginines [2,6,51]. Similar results were obtained by Björnerås and coworkers [11] for bicelles by circular dichroism and nuclear magnetic resonance (NMR) spectroscopy.

4. Conclusions

By means of electrophysiological experiments, we show that DynA generates two kinds of permeabilization events in neutral membranes. On the one side, ion channel-like pores similar to those previously reported are observed in charged membranes. On the other side, unprecedented events thermodynamically incompatible with voltage-driven transport in passive pores are obtained (i.e. currents without applied voltage, selectivity calculated from the reversal potential that goes beyond the theoretical limit) that we ascribe to DynA direct translocation. The coexistence of voltage-driven transport corresponding to first-order kinetics with translocation phenomena ruled by zero-order kinetics is revealed through uncorrelated fluctuation patterns. By comparison with another translocating amphiphilic molecule (metallacarborane [*o*-COSAN]$^-$) that can be assessed by analytical techniques, we hypothesize that DynA translocation occurs via a mechanism that includes absorption/reorientation/desorption steps in which the amphiphilic properties of the peptide and the membrane composition play a capital role in agreement with previous experimental and computational studies. Understanding how peptides with specific properties (CPPs, antimicrobial peptides, etc.) can cross biological membranes without the help of cellular machinery is essential for the rational design of novel therapeutics where translocating peptides could be used directly or as carriers of other complexes [45].

Declaration of Competing Interest

The authors declare that they have no known competing financial interests or personal relationships that could have appeared to influence the work reported in this paper.

Data availability

Data will be made available on request.

Acknowledgements

Authors acknowledge financial support by the Spanish Government MCIN/AEI/ 10.13039/501100011033 (Project 2019-108434GB-I00 to A.A., Project IJC2018-035283-I to M.Q.M. and Project PID2020-120222GB-I00 to A.P.-M.) and Universitat Jaume I (Project UJI-B2022-42 to A.A. and UJI-A2020-21 to M.Q.M).

Appendix A. Supplementary material

Supplementary data to this article can be found online at https://doi.org/10.1016/j.bioelechem.2023.108527.

References

[1] K.F. Hauser, J.V. Aldrich, K.J. Anderson, G. Bakalkin, M.J. Christie, E.D. Hall, P. E. Knapp, S.W. Scheff, I.N. Singh, B. Vissel, A.S. Woods, T. Yakovleva, T. S. Shippenberg, Pathobiology of dynorphins in trauma and disease, Front. Biosci. 10 (2005) 216–235, https://doi.org/10.2741/1522.
[2] L. Hugonin, V. Vukojević, G. Bakalkin, A. Gräslund, Calcium influx into phospholipid vesicles caused by dynorphin neuropeptides, Biochim. Biophys. Acta. 1778 (2008) 1267–1273, https://doi.org/10.1016/j.bbamem.2008.02.003.
[3] K. Tan-No, G. Cebers, T. Yakovleva, B. Hoon Goh, I. Gileva, K. Reznikov, M. Aguilar-Santelises, K.F. Hauser, L. Terenius, G. Bakalkin, Cytotoxic Effects of Dynorphins through Nonopioid Intracellular Mechanisms, Exp. Cell Res. 269 (2001) 54–63, https://doi.org/10.1006/excr.2001.5309.

[4] C.J.L.M. Smeets, J. Zmorzyńska, M.N. Melo, A. Stargardt, C. Dooley, G. Bakalkin, J. McLaughlin, R.J. Sinke, S.-J. Marrink, E. Reits, D.S. Verbeek, Altered secondary structure of Dynorphin A associates with loss of opioid signalling and NMDA-mediated excitotoxicity in SCA23, Hum. Mol. Genet. (2016) ddw130, https://doi.org/10.1093/hmg/ddw130.

[5] K. Tan-No, H. Takahashi, O. Nakagawasai, F. Niijima, S. Sakurada, G. Bakalkin, L. Terenius, T. Tadano, Chapter 15 Nociceptive Behavior Induced by the Endogenous Opioid Peptides Dynorphins in Uninjured Mice, in: Evidence with Intrathecal N-Ethylmaleimide Inhibiting Dynorphin Degradation, 1st ed.,, Elsevier Inc., 2009, https://doi.org/10.1016/S0074-7742(09)85015-0.

[6] F. Madani, M.M. Taqi, S.K.T.S. Wärmländer, D.S. Verbeek, G. Bakalkin, A. Gräslund, Perturbations of model membranes induced by pathogenic dynorphin A mutants causing neurodegeneration in human brain, Biochem. Biophys. Res. Commun. 411 (2011) 111–114, https://doi.org/10.1016/j.bbrc.2011.06.105.

[7] D.A. Perini, M. Aguilella-Arzo, A. Alcaraz, A. Perálvarez-Marín, M. Queralt-Martín, Dynorphin A induces membrane permeabilization by formation of proteolipidic pores. Insights from electrophysiology and computational simulations, Comput. Struct, Biotechnol. J. 20 (2022) 230–240, https://doi.org/10.1016/j.csbj.2021.12.021.

[8] R.J.C. Gilbert, M.D. Serra, C.J. Froelich, M.I. Wallace, G. Anderluh, Membrane pore formation at protein–lipid interfaces, Trends Biochem. Sci. 39 (2014) 510–516, https://doi.org/10.1016/j.tibs.2014.09.002.

[9] V.M. Aguilella, C. Verdiá-Báguena, A. Alcaraz, Lipid charge regulation of non-specific biological ion channels, Phys. Chem. Chem. Phys. 16 (2014) 3881–3893, https://doi.org/10.1039/c3cp54690j.

[10] Z. Marinova, V. Vukojević, S. Surcheva, T. Yakovleva, G. Cebers, N. Pasikova, I. Usynin, L. Hugonin, W. Fang, M. Hallberg, D. Hirschberg, T. Bergman, Ü. Langel, K.F. Hauser, A. Pramanik, J.V. Aldrich, A. Gräslund, L. Terenius, G. Bakalkin, Translocation of dynorphin neuropeptides across the plasma membrane: A putative mechanism of signal transmission, J. Biol. Chem. 280 (2005) 26360–26370, https://doi.org/10.1074/jbc.M412494200.

[11] J. Björnerås, A. Gräslund, L. Mäler, Membrane interaction of disease-related dynorphin A variants, Biochemistry. 52 (2013) 4157–4167, https://doi.org/10.1021/bi4004205.

[12] J. Lind, A. Gräslund, L. Mäler, Membrane Interactions of Dynorphins, Biochemistry. 45 (2006) 15931–15940, https://doi.org/10.1021/bi061199g.

[13] H. Derakhshankhah, S. Jafari, Cell penetrating peptides: A concise review with emphasis on biomedical applications, Biomed. Pharmacother. 108 (2018) 1090–1096, https://doi.org/10.1016/j.biopha.2018.09.097.

[14] F.G. Avci, B.S. Akbulut, E. Ozkirimli, Membrane Active Peptides and Their Biophysical Characterization, Biomolecules. 8 (2018) 77, https://doi.org/10.3390/biom8030077.

[15] M. Di Pisa, G. Chassaing, J.-M. Swiecicki, Translocation Mechanism(s) of Cell-Penetrating Peptides: Biophysical Studies Using Artificial Membrane Bilayers, Biochemistry. 54 (2015) 194–207, https://doi.org/10.1021/bi501392n.

[16] E. Bárány-Wallje, S. Keller, S. Serowy, S. Geibel, P. Pohl, M. Bienert, M. Dathe, A Critical Reassessment of Penetratin Translocation Across Lipid Membranes, Biophys. J. 89 (2005) 2513–2521, https://doi.org/10.1529/biophysj.105.067694.

[17] P.G. Dougherty, A. Sahni, D. Pei, Understanding Cell Penetration of Cyclic Peptides, Chem. Rev. 119 (2019) 10241–10287, https://doi.org/10.1021/acs.chemrev.9b00008.

[18] Z. Marinova, Opioid and non-opioid activities of the dynorphins. Ph.D. Thesis. Department of Clinical Neuroscience. Karolinska Institutet. https://openarchive.ki.se/xmlui/handle/10616/38572.

[19] D.C. Malaspina, C. Viñas, F. Teixidor, J. Faraudo, Atomistic Simulations of COSAN: Amphiphiles without a Head-and-Tail Design Display “Head and Tail” Surfactant Behavior, Angew. Chemie - Int. Ed. (2020) 1–6. https://doi.org/10.1002/anie.201913257.

[20] C. Verdiá-Báguena, A. Alcaraz, V.M. Aguilella, A.M. Cioran, S. Tachikawa, H. Nakamura, F. Teixidor, C. Viñas, Amphiphilic COSAN and I2-COSAN crossing synthetic lipid membranes: planar bilayers and liposomes, Chem. Commun. (Camb) 50 (2014) 6700–6703, https://doi.org/10.1039/c4cc01283f.

[21] S.M. Bezrukov, I. Vodyanoy, Probing alamethicin channels with water-soluble polymers. Effect on conductance of channel states, Biophys. J. 64 (1993) 16–25, https://doi.org/10.1016/S0006-3495(93)81336-5.

[22] M. Montal, P. Mueller, Formation of bimolecular membranes from lipid monolayers and a study of their electrical properties, Proc. Natl. Acad. Sci. U. S. A. 69 (1972) 3561–3566, https://doi.org/10.1073/pnas.69.12.3561.

[23] A. Zaulet, F. Teixidor, P. Bauduin, O. Diat, P. Hirva, A. Ofori, C. Viñas, Deciphering the role of the cation in anionic cobaltabisdicarbollide clusters, J. Organomet. Chem. 865 (2018) 214–225, https://doi.org/10.1016/J.JORGANCHEM.2018.03.023.

[24] A. Alcaraz, E.M. Nestorovich, M.L. López, E. García-Giménez, S.M. Bezrukov, V. M. Aguilella, Diffusion, Exclusion, and Specific Binding in a Large Channel: A Study of OmpF Selectivity Inversion, Biophys. J. 96 (2009) 56–66, https://doi.org/10.1016/j.bpj.2008.09.024.

[25] M.L. López, M. Aguilella-Arzo, V.M. Aguilella, A. Alcaraz, Ion selectivity of a biological channel at high concentration ratio: Insights on small ion diffusion and binding, J. Phys. Chem. B. 113 (2009) 8745–8751, https://doi.org/10.1021/jp902267g.

[26] C. Verdiá-Báguena, M. Queralt-Martín, V.M. Aguilella, A. Alcaraz, Protein ion channels as molecular ratchets. Switchable current modulation in outer membrane protein F porin induced by millimolar La 3+ ions, J. Phys. Chem. C. 116 (2012) 6537–6542, https://doi.org/10.1021/jp210790r.

[27] G.C. Fadda, D. Lairez, G. Zalczer, Fluctuations of Ionic Current Through Lipid Bilayers at the Onset of Peptide Attacks and Pore Formation, Phys. Rev. Lett. 103 (2009), https://doi.org/10.1103/PhysRevLett.103.180601.

[28] E. Gazit, A. Boman, H.G. Boman, Y. Shai, Interaction of the Mammalian Antibacterial Peptide Cecropin PI with Phospholipid Vesicles, Biochemistry. 34 (1995) 11479–11488, https://doi.org/10.1021/bi00036a021.

[29] R.O. Blaustein, On the Impossibility of Nonzero Reversal Potentials of Passive Pores Separating Symmetric Solutions: Comment on Haemophilus influenzae Outer Membrane Protein P5 Is Associated with Inorganic Polyphosphate and Polyhydroxybutyrate, Biophys. J. 93 (2007) 2978, https://doi.org/10.1529/biophysj.107.104919.

[30] E. Zakharian, R.N. Reusch, Haemophilus influenzae outer membrane protein P5 is associated with inorganic polyphosphate and polyhydroxybutyrate, Biophys. J. 92 (2007) 588–593, https://doi.org/10.1529/biophysj.106.095273.

[31] E. Largo, M. Queralt-Martín, P. Carravilla, J.L. Nieva, A. Alcaraz, Single-molecule conformational dynamics of viroporin ion channels regulated by lipid-protein interactions, Bioelectrochemistry. 137 (2021), 107641, https://doi.org/10.1016/j.bioelechem.2020.107641.

[32] S.M. Bezrukov, I. Vodyanoy, Noise in Biological Membranes and Relevant Ionic Systems, in: 1994: pp. 375–399. https://doi.org/10.1021/ba-1994-0235.ch017.

[33] B. Neumcke, 1/f noise in membranes, Biophys. Struct. Mech. 4 (1978) 179–199, https://doi.org/10.1007/BF02426084.

[34] Z.S. Siwy, A. Fuliński, Origin of 1/f(alpha) noise in membrane channel currents, Phys. Rev. Lett. 89 (2002), 158101, https://doi.org/10.1103/PhysRevLett.89.158101.

[35] S.M. Bezrukov, M. Winterhalter, Examining Noise Sources at the Single-Molecule Level: 1/f Noise of an Open Maltoporin Channel, Phys. Rev. Lett. 85 (2000) 202–205, https://doi.org/10.1103/PhysRevLett.85.202.

[36] P. Bak, C. Tang, K. Wiesenfeld, Self-organized criticality: An explanation of the 1/ f noise, Phys. Rev. Lett. 59 (1987) 381–384, https://doi.org/10.1103/PhysRevLett.59.381.

[37] E. Rigo, Z. Dong, J.H. Park, E. Kennedy, M. Hokmabadi, L. Almonte-Garcia, L. Ding, N. Aluru, G. Timp, Measurements of the size and correlations between ions using an electrolytic point contact, Nat. Commun. 10 (2019), https://doi.org/10.1038/s41467-019-10265-2.

[38] C. Tasserit, A. Koutsioubas, D. Lairez, G. Zalczer, M.C. Clochard, Pink noise of ionic conductance through single artificial nanopores revisited, Phys. Rev. Lett. 105 (2010), https://doi.org/10.1103/PhysRevLett.105.260602.

[39] D.P. Hoogerheide, S. Garaj, J.A. Golovchenko, Probing surface charge fluctuations with solid-state nanopores, Phys. Rev. Lett. 102 (2009), 256804, https://doi.org/10.1103/PhysRevLett.102.256804.

[40] M. Queralt-Martín, D.A. Perini, A. Alcaraz, Specific adsorption of trivalent cations in biological nanopores determines conductance dynamics and reverses ionic selectivity, Phys. Chem. Chem. Phys. 23 (2021) 1352–1362, https://doi.org/10.1039/D0CP04486E.

[41] N. Laksminarayanaiah. Transport phenomena in membranes, Academic Press, New York, 1969 https://scholar.google.com/scholar_lookup?title=Transport%20phenomena%20in%20membranes&author=N.%20Laksminarayanaiah&publication_year=1969.

[42] B. Hille. Ion Channels of Excitable Membranes, Third Ed., Sinauer Associates Inc, Sunderland, MA, MA, 2001 https://scholar.google.com/scholar_lookup?hl=en&publication_year=2001&author=B.+Hille&title=Ion+Channels+of+Excitable+Membraneshttp://www.sinauer.com/ion-channels-of-excitable-membranes.html#.UvDS-CVNRd8.mendeley.

[43] S.A. Spinella, R.B. Nelson, D.E. Elmore, Measuring Peptide Translocation into Large Unilamellar Vesicles, J. Vis. Exp. (2012), https://doi.org/10.3791/3571.

[44] M.-L. Jobin, I.D. Alves, Label-free quantification of cell-penetrating peptide translocation into liposomes, Anal. Methods. 8 (2016) 4608–4616, https://doi.org/10.1039/C6AY00719H.

[45] I. Kabelka, R. Vácha, Optimal Hydrophobicity and Reorientation of Amphiphilic Peptides Translocating through Membrane, Biophys. J. 115 (2018) 1045–1054, https://doi.org/10.1016/j.bpj.2018.08.012.

[46] S.A. Hassan, E.L. Mehler, D. Zhang, H. Weinstein, Molecular dynamics simulations of peptides and proteins with a continuum electrostatic model based on screened Coulomb potentials, Proteins Struct. Funct. Genet. 51 (2003) 109–125, https://doi.org/10.1002/prot.10330.

[47] R. Sankararamakrishnan, H. Weinstein, Molecular dynamics simulations predict a tilted orientation for the helical region of dynorphin A(1–17) in dimyristoylphosphatidylcholine bilayers, Biophys. J. 79 (2000) 2331–2344, https://doi.org/10.1016/S0006-3495(00)76479-4.

[48] R. Sankararamakrishnan, H. Weinstein, Positioning and Stabilization of Dynorphin Peptides in Membrane Bilayers: the Mechanistic Role of Aromatic and Basic Residues Revealed from Comparative MD Simulations, J. Phys. Chem. B. 106 (2002) 209–218, https://doi.org/10.1021/jp012174o.

[49] A. Kira, N. Javkhlantugs, T. Miyamori, Y. Sasaki, M. Eguchi, I. Kawamura, K. Ueda, A. Naito, Interaction of extracellular loop II of κ-opioid receptor (196–228) with opioid peptide dynorphin in membrane environments as revealed by solid state nuclear magnetic resonance, quartz crystal microbalance and molecular dynamics simulation, J. Phys. Chem. B. 118 (2014) 9604–9612, https://doi.org/10.1021/jp505412j.

[50] A. Dehsorkhi, V. Castelletto, I.W. Hamley, Self-assembling amphiphilic peptides, J. Pept. Sci. 20 (2014) 453–467, https://doi.org/10.1002/psc.2633.

[51] L. Hugonin, V. Vukojević, G. Bakalkin, A. Gräslund, Membrane leakage induced by dynorphins, FEBS Lett. 580 (2006) 3201–3205, https://doi.org/10.1016/j.febslet.2006.04.078.